J Neurophysiol 98: 1213–1222, 2007.
First published July 25, 2007; doi:10.1152/jn.00493.2007.

Characterization of the Heteromeric Potassium Channel Formed by Kv2.1 and the Retinal Subunit Kv8.2 in *Xenopus* Oocytes

Gábor Czirják,[1] Zsuzsanna E. Tóth,[2] and Péter Enyedi[1]

[1]*Department of Physiology, Semmelweis University; and* [2]*Neuromorphological and Neuroendocrine Research Laboratory, Department of Anatomy, Histology and Embryology, Semmelweis University and the Hungarian Academy of Sciences, Budapest, Hungary*

Submitted 2 May 2007; accepted in final form 19 July 2007

Czirják G, Tóth ZE, Enyedi P. Characterization of the heteromeric potassium channel formed by Kv2.1 and the retinal subunit Kv8.2 in *Xenopus* oocytes. *J Neurophysiol* 98: 1213–1222, 2007. First published July 25, 2007; doi:10.1152/jn.00493.2007. Kv8.2 (KCNV2) subunits do not form homotetrameric potassium channels, although they coassemble with Kv2.1 to constitute functional heteromers. High expression of Kv8.2 was reported in the human retina and its mutations were linked to the visual disorder "cone dystrophy with supernormal rod electroretinogram." We detected abundant Kv8.2 expression in the photoreceptor layer of mouse retina, where Kv2.1 is also known to be present. When the two subunits were coexpressed in *Xenopus* oocytes in equal amounts, Kv8.2 abolished the current of Kv2.1. If the proportion of Kv8.2 was reduced then the current of heteromeric channels emerged. Kv8.2 shifted the steady-state activation of Kv2.1 to more negative potentials, without affecting the voltage dependence of inactivation. This gave rise to a window current within the −40 to −10 mV membrane potential range. Ba^{2+} inhibited the heteromeric channel and shifted its activation to more positive potentials. These electrophysiological and pharmacological properties resemble those of the voltage-gated K^+ current (named I_{Kx}) described in amphibian retinal rods. Furthermore, oocytes expressing Kv2.1/Kv8.2 developed transient hyperpolarizing overshoots in current-clamp experiments, whereas those expressing only Kv2.1 failed to do so. Similar overshoots are characteristic responses of photoreceptors to light flashes. We demonstrated that Kv8.2 G476D, analogous to a disease-causing human mutation, eliminated Kv2.1 current, if the subunits were coexpressed equally. However, Kv8.2 G476D did not form functional heteromers under any conditions. Therefore we suggest that the custom-tailored current of Kv2.1/Kv8.2 functionally contributes to photoreception, and this is the reason that mutations of Kv8.2 lead to a genetic visual disorder.

INTRODUCTION

Voltage-gated K^+ channels selectively transfer potassium ions through the plasma membrane in response to depolarization. The ion-conducting core of voltage-gated K^+ channels is composed of four Kvα subunits, which also possess the voltage sensor. According to structural similarities, members of the Kv family were initially divided into four subfamilies (Kv1–Kv4), the mammalian equivalents of the *Drosophila Shaker*, *Shab*, *Shaw*, and *Shal* gene products, respectively. These Kv subunits give rise to functional homotetrameric K^+ channels, when they are expressed heterologously in *Xenopus laevis* oocytes (for review see Coetzee et al. 1999). Coexpression of members of the same subfamily may result in functional heterotetrameric channels and currents with properties different from those of the homotetramers of the parent subunits. The current of these heteromeric Kv channels was also identified in native tissues (Sheng et al. 1993; Wang et al. 1993). Subunits belonging to different Kv1–Kv4 subfamilies do not coassemble. The selectivity within the subfamilies is ensured by the specific N-terminal tetramerization domains (Li et al. 1992; Shen and Pfaffinger 1995).

The Kv2 (*Shab*) subfamily, which is known to participate in the formation of channels underlying delayed rectifier currents, contains only two members (Kv2.1 and Kv2.2, also called KCNB1 and KCNB2, respectively). Still, the delayed rectifying potassium currents show remarkable variability in different tissues. The discovery of further modulatory subunits helped to explain this diversity. Members of the Kv5–Kv9 families apparently have all the structural hallmarks of a functioning K^+ channel α-subunit, yet they do not induce K^+ currents, if they are expressed by themselves in *Xenopus* oocytes. On the other hand, these so-called silent or γ-subunits can combine with members of the delayed rectifier Kv2 subfamily to form channels with distinct properties. Coexpression of silent Kv subunits reduces the amplitude of Kv2 current in general (Hugnot et al. 1996; Salinas et al. 1997a,b), whereas in the case of Kv9.3 both increased (Patel et al. 1997) and suppressed Kv2.1 currents have been reported (Stocker et al. 1999). Modification of the activation, inactivation, deactivation kinetics (Patel et al. 1997; Post et al. 1996; Salinas et al. 1997b; Stocker et al. 1999) and other gating properties (Kramer et al. 1998) of Kv2.1 by the silent subunits have also been described. These heteromeric delayed rectifiers may shape the action potentials and other electrophysiological processes according to the special "need" of the particular cell type.

The silent potassium channel subunit Kv8.2 was cloned from human testis cDNA and its expression was detected by reverse transcriptase polymerase chain reaction (RT-PCR) in different tissues (Ottschytsch et al. 2002). (Originally, the Kv11.1 name was used to describe the KCNV2 gene product instead of Kv8.2. However, later the Kv11.1 name was reassigned to another, more extensively studied K^+ channel subunit, HERG, and this nomenclature has become widely accepted since then. Therefore we follow the guidelines of the HUGO Gene Nomenclature Committee and describe the KCNV2 gene product as Kv8.2 in this article.) Kv8.2 did not form functional channels by itself but heteromerized with Kv2.1 in coexpression experiments (Ottschytsch et al. 2002). In pulmonary artery smooth muscle cells, an apoptotic signal

Address for reprint requests and other correspondence: P. Enyedi, Dept. of Physiology, Semmelweis University of Medicine, P.O. Box 259, Budapest, Hungary H-1444 (E-mail: enyedi@puskin.sote.hu).

The costs of publication of this article were defrayed in part by the payment of page charges. The article must therefore be hereby marked "*advertisement*" in accordance with 18 U.S.C. Section 1734 solely to indicate this fact.

(bone morphogenic protein 2) powerfully downregulated Kv8.2 expression, but simultaneously upregulated the expression of several other Kv channel subunits. Therefore a constitutive inhibitory role was proposed for Kv8.2. According to this hypothesis, the alleviation of Kv8.2 expression may contribute to the increased Kv channel activity (Fantozzi et al. 2006). In a recent publication, mutation of the KCNV2 (Kv8.2) gene was linked to an autosomal recessive disorder "cone dystrophy with supernormal rod electroretinogram." Moreover, a high level of Kv8.2 expression was detected in the photoreceptor layer of the human retina (Wu et al. 2006). The absence of any other apparent phenotypic consequence in addition to the retinal impairment in these patients strongly suggested that the silent Kv8.2 subunit may have a pivotal and unique role in the photoreceptor cells.

Retinal photoreceptor cells have an exceptional electrical response system. A persistent inward current through cyclic-nucleotide–gated (CNG) channels in the outer segment keeps the cells in a depolarized state in the dark. Light stimulus evokes rapid reduction of the cytoplasmic cyclic guanosine 3′,5′-monophosphate (cGMP) concentration and the closure of CNG channels, which hyperpolarizes the membrane and decreases transmitter release. A special property of this electrical response system is the generation of amplified membrane potential alterations in response to rapid changes of inward current (induced by light). The onset of light evokes a transient augmented hyperpolarization, which exceeds the hyperpolarization obtained during sustained illumination. This dynamic response enhances the sensitivity of photoreceptor cells to the changes of light intensity. The mechanism responsible for the transient overhyperpolarization was examined first in amphibian photoreceptors and it was principally attributed to an undefined voltage-dependent potassium current (I_{Kx}) (Beech and Barnes 1989).

We have cloned Kv8.2 subunit from mouse retina and expressed the channel in *Xenopus* oocytes. Our studies revealed previously unrealized electrophysiological and pharmacological properties of the Kv2.1/Kv8.2 heteromer. We have demonstrated that unlike Kv2.1, the Kv2.1/Kv8.2 heteromer provides a sustained current in the membrane potential range characteristic for photoreceptor cells. This sustained current and the slow deactivation are the two essential electrophysiological features that enable the heteromer to produce transient hyperpolarization after the cessation of a continuous inward current. Furthermore, we report that a pore domain mutant of Kv8.2 can reduce the amplitude, but does not transform the characteristics of the Kv2.1 current, like the wild-type subunit does. Because the corresponding human pore domain mutation resulted in a disease similar to that caused by the complete loss of Kv8.2 (Wu et al. 2006), we suggest that it is the Kv2.1/Kv8.2 current, and not merely the downregulation of Kv2.1, that is necessary for the appropriate photoreceptor cell function.

METHODS

Materials

Enzymes and kits for molecular biological studies were purchased from Ambion (Austin, TX), Amersham (Little Chalfont, UK), Fermentas (Vilnius, Lithuania), Invitrogen (Carlsbad, CA), New England Biolabs (Beverly, MA), Pharmacia Biotech (Uppsala, Sweden), Promega (Madison, WI), Qiagen (Chatworth, CA), and Stratagene (La Jolla, CA). Fine chemicals of analytical grade were obtained from Fluka (Buchs, Switzerland), Promega, and Sigma Chemical (St. Louis, MO). [α-^{35}S]UTP was from NEN (Budapest, Hungary).

RNA preparation, RT-PCR, and cloning of mouse Kv8.2

Total RNA was prepared from different mouse tissues by the guanidium-isothiocyanate, phenol-chloroform method as previously described (Horváth et al. 1998). For RT-PCR reactions total RNA was reverse transcribed by MMLV (mouse Moloney leukemia virus) or GIBCO Superscript II reverse transcriptase. The 5′ end of the Kv8.2 coding sequence was amplified with Pfu DNA polymerase from mouse eye total RNA after reverse transcription. The forward primer was 5′-CAG gaa ttc CCA CCA CCA TGC TGA AAC-3′ (containing an upstream *Eco* RI site for cloning and the mRNA sequence from bases −8 to 10); the reverse primer was 5′-GCC CAC CTG CTG GTA GCA CTGG-3′ (1,266–1,287). The Kv8.2 coding region was assembled from this PCR product and the BG342392 mouse retina expressed sequence tag (EST; taking advantage of the overlapping Eco72I site at position 936) and subcloned into the pEXO vector, between the 5′- and 3′-untranslated regions of *Xenopus* globin gene. The sequence of the construct (pEXO-mouseKv8.2) was verified by sequencing.

For detection of the Kv8.2 message in different mouse tissues by RT-PCR the forward primer was 5′-GCA GGG CAG TGT ACT CTC CAGG-3′ [(−72)–(−51)]; the reverse primer was 5′-CCT CCG GAT GGC GGT GTA CTCG-3′ (1,569–1,590). DNA was amplified with HotStar *Taq* [initial denaturation and HotStar *Taq* activation for 14 min at 94°C; 40 cycles of denaturation for 1 min at 94°C, annealing for 1 min, and extension for 2 min at 72°C; followed by 7-min final extension at 72°C. Annealing temperatures were 64, 62, and 60°C for the first 3 × 5 cycles and 58°C for the final 25 cycles (touchdown PCR)].

In vitro site-directed mutagenesis

In vitro site-directed mutagenesis was performed according to the manufacturer's instructions using the QuikChange Site-Directed Mutagenesis Kit (Stratagene). Complementary primer pairs were designed coding for the desired G476D mutation of pEXO-mouseKv8.2 together with a nearby silent mutation (introducing a discriminating *Sal* I restriction enzyme site). The forward primer was 5′-AGC ATC TCC ACC GTc GaC TAT GGA GAC ATG TAC-3′ (differences from the original sequence are indicated by lowercase letters).

In situ hybridization

A DNA fragment corresponding to the unique N-terminus of Kv8.2 was PCR-amplified from our pEXO-mouseKv8.2 plasmid with the forward primer annealing to the start codon (see preceding text) and the reverse primer 5′-GCT GGA GTA TCG TTG TGG CC-3′ (286–305). The PCR product was cloned into Bluescript II pKS- vector between *Eco* RI and *Eco* RV restriction sites. The probe template for in situ hybridizations was PCR-amplified from this clone applying the T7 and T3 promoter primers. The template was in vitro transcribed (MaxiScript kit, Ambion) to radioactively labeled sense and antisense RNA probes, using T7 and T3 RNA polymerases, respectively.

The in situ hybridization was performed as described previously (Bradley et al. 1992; Young 3rd 1989). The tissues (mice eyes and whole rat pups) were frozen on dry ice and 12-μm-thick parasagittally directed sections were cut on a cryostat. The sections were thaw-mounted and air dried at 37°C onto positively charged Superfrost Plus slides (Fisher Scientific, Pittsburgh, PA), frozen, and stored at −80°C. The sections were fixed in 4% formaldehyde in PBS (pH 7.4) for 10 min at room temperature. The fixative was washed out in PBS (2 ×

5 min), and the slides were treated with 0.25% acetic anhydride in 0.1 mol/l triethanolamine-HCl (pH 8.0) for an additional 10 min. The sections were rinsed with 1× SSC, dehydrated and delipidated in 70–85–95–100% ethanol, and air dried. The sections were hybridized overnight at 55°C with 10^6 cpm/section radioactively labeled sense or antisense riboprobes in a humid chamber. The following day the sections were washed in 4× SSC solution (pH 7.0) for 4 × 5 min at room temperature, in a buffer containing 20 μg/ml RNase A for 30 min at 37°C, in 2×, 1×, and 0.5× SSC solutions for 5 min at room temperature, and in 0.1× SSC solution for 2 × 30 min at 65°C. After washing, the slides were dehydrated again in 70–85–95% ethanol and air dried. The reaction was checked on Kodak Biomax MR film exposed for 3 days and the slides were dipped into NTB3 nuclear track emulsion (Eastman Kodak, Rochester, NY). The reaction was developed after 10 days of incubation in the dark at 4°C using Kodak Dektol developer and the tissue was counterstained with 0.5% Giemsa solution. The sections were dried again and coverslipped using Cytoseal 60 mounting medium (Stephens Scientific, Riverdale, NJ).

In vitro RNA synthesis for Xenopus oocyte injection

Coding RNAs of mouse Kv8.2, rat Kv2.1, GIRK4m [S143T mutant of GIRK4 (also called Kir3.4), which can constitute functional channels even in the absence of other GIRK subunits (Vivaudou et al. 1997)], and human TASK-1 (KCNK3) potassium channels were synthesized in vitro according to the manufacturer's instructions (Ambion mMESSAGE mMACHINE T7 In vitro Transcription Kit). The templates were the pEXO-mouseKv8.2, pCIrKv2.1, pGEMHE-GIRK4-S143T, and pEXO-TASK-1 (Duprat et al. 1997) constructs, linearized by *Xba* I or *Not* I restriction enzymes.

Animals, tissue preparation, and Xenopus oocyte injection

Mature female *Xenopus laevis* frogs were obtained from Amrep Reptielen (Breda, Netherlands). Defolliculated oocytes were prepared as previously described (Czirják and Enyedi 2002) and they were injected one day after defolliculation. Fifty nanoliters of the appropriate RNA solution was delivered with Nanoliter Injector (World Precision Instruments, Saratosa, FL). The injected solution contained 0.03–2 ng of the different RNAs. [For expression of the Kv2.1/Kv8.2 heteromer, the upper values of the range were used, whereas (in the same experiment) the group of cells expressing Kv2.1 currents of similar amplitude were selected from several groups injected with different dilutions corresponding to the lower values of this range.] Electrophysiological experiments were performed 3 or 4 days after the injection.

The tissues for RNA preparation and in situ hybridization derived from NMRI mice (Toxicop, Budapest, Hungary) and 6-day-old Wistar rat pups. All treatment of the animals was conducted in accordance with state laws and institutional regulations. The experiments were approved by the Animal Care and Ethics Committee of Semmelweis University.

Electrophysiology

Voltage-clamp measurements were performed by two-electrode voltage clamp (OC-725-C; Warner Instrument, Hamden, CT) using microelectrodes made of borosilicate glass (Clark Electromedical Instruments, Pangbourne, UK) with resistance of 0.3–1 MΩ when filled with 3 M KCl. Currents were filtered at 1 kHz, digitally sampled at 1–2.5 kHz with a Digidata Interface (Axon Instruments, Foster City, CA). For current-clamp measurements, membrane potential was recorded by the voltage section of OC-725-C connected to another analog in channel of Digidata 1200, and current was injected through a third microelectrode inserted additionally into the oocyte. This microelectrode was connected to a custom-designed current-clamp electronics. This setup allowed easy switching between two-electrode voltage-clamp recording and two-electrode current-clamp recording in the same oocyte. Recording and data analysis were performed using pCLAMP software 6.0 (Axon Instruments). Experiments were carried out at room temperature, and solutions were applied by a gravity-driven perfusion system. Low [K^+] solution contained (in mM): NaCl 95.4, KCl 2, $CaCl_2$ 1.8, HEPES 5. High [K^+] solution contained 80 mM K^+ (78 mM Na^+ of the low [K^+] solution was replaced with K^+). The pH of the solutions was adjusted to 7.5 with NaOH. The blocking ions (Cs^+, Cd^{2+}, Ba^{2+}, and Ca^{2+}) were included in the solution without changing the concentration of other components.

Steady-state activation of the potassium channels was estimated by measuring the tail-current amplitudes at −40 mV after 200-ms activating prepulses to different potentials. The steady-state inactivation of the currents was measured in the same oocytes by forcing maximal activation at +60 mV after 1-min inactivation at different potentials. The kinetics of activation (and its voltage dependence) was estimated by fitting the time course of activation (during voltage steps from −80 mV to different potentials) with monoexponentials. Closed-state inactivation was measured according to Kerschensteiner and Stocker (1999). Briefly, a 200-ms test pulse (P1) to +40 mV was followed by a depolarization to −30 or −50 mV for 1–12 s (P2). These applied voltages of P2 were 10 mV more negative than the activation threshold of Kv2.1 and Kv2.1/Kv8.2, respectively. P2 was followed by a second 200-mV pulse to +40 mV (P3). Closed-state inactivation was calculated as the ratio of the currents measured during P3 and P1 and it was presented as a function of the duration of P2.

Statistics and calculations

Data are expressed as means ± SE. Statistical significance was estimated by *t*-test for independent samples or two-way, repeated-measures ANOVA using Statistica 6.0 (Statsoft, Tulsa, OK). The difference was considered to be significant at $P < 0.05$. Nonlinear curve fitting was performed with Clampfit 6.0 [Minimax error minimalization, mixed-fit method (Chebyshev method followed by simplex iterations)] or Origin 6.0 (using sum-of-squares error minimalization and simplex iterations; Microcal, Northampton, MA). The functions were $A_1 \times \exp[-(t - T)/\tau] + C$ for monoexponential and $A_2/\{1 + \exp[(E - V_{1/2})/k]\} + C$ for Boltzmann fit, where A_1 and A_2 are the amplitudes, τ is the time constant, T is the start of fit, E is the membrane potential, $V_{1/2}$ is the voltage of half-maximal activation (or inactivation), k is the slope of voltage dependence, and C is constant (offset). For fitting normalized steady-state activation and inactivation $A_2 = -1$, $C = 1$ and $A_2 = 1$, $C = 0$ were forced, respectively. Kv2.1 (and Kv2.1/Kv8.2) activation at the activation threshold was not well fitted with a Boltzmann function, similarly to the results of others (Stocker and Kerschensteiner 1998).

RESULTS

Cloning of mouse Kv8.2

The 5′ end of the coding region was amplified by RT-PCR from mouse eye total RNA with primers designed on the basis of EST data. A retinal EST clone (BG342392) containing the 3′ end of the coding region of mouse Kv8.2 was purchased from I.M.A.G.E. Consortium. The full-length channel cDNA was assembled from the PCR product and BG342392 EST clone and its sequence was determined and deposited to GenBank (Accession No. AY238939).

Localization of Kv8.2 mRNA in mouse tissues

Kv8.2 mRNA expression was detected in different mouse tissues by RT-PCR. Intron spanning oligonucleotides were designed to avoid the amplification of genomic sequences. A

large amount of the PCR product was amplified from eye and heart (Fig. 1). Under identical conditions, the product of appropriate size [1,662 base pairs (bp)] was also amplified from lung, cerebellum, and cerebrum, but in these tissues much fainter bands were obtained. Specificity of the 1,662-bp PCR product was verified by restriction enzyme mapping (not shown).

The distribution of Kv8.2 in different tissues was also examined by in situ hybridization. Kv8.2-specific, radioactively labeled antisense RNA probe (corresponding to the unique N-terminus of the channel) was hybridized to a parasagittal section of a whole perinatal rat. This in situ hybridization demonstrated by far the highest expression in the eye (Fig. 2*A*). The experiment was also performed with sagittal sections of isolated adult mouse eyes. Kv8.2 was localized to the outer nuclear layer (ONL) of the retina (Fig. 2*B*). All of the in situ hybridizations were also performed with the sense (control) RNA probe, and these experiments failed to give any signal, or only a faint homogeneous distribution was obtained (Fig. 2*C*).

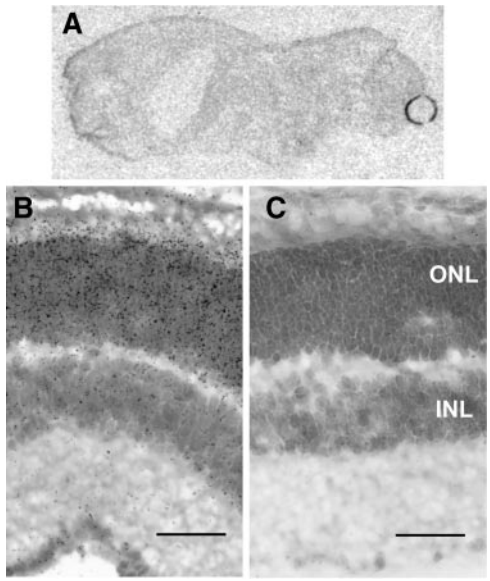

FIG. 2. Kv8.2 signal is detected in the outer nuclear layer of rodent retina by in situ hybridization. *A*: in situ hybridization on a parasagittal section of a whole perinatal rat using Kv8.2-specific radioactively labeled antisense RNA probe. Only the eye shows specific labeling. *B*: Kv8.2 in situ hybridization of a mouse retina section with the antisense RNA probe. Note the high grain density above the outer nuclear layer. *C*: control in situ hybridization with sense Kv8.2 RNA probe. ONL, outer nuclear layer; INL, inner nuclear layer. Scale bar represents 50 μm.

Heterologous expression of mouse Kv8.2 in Xenopus laevis oocytes

The currents of *Xenopus* oocytes injected with Kv8.2 synthetic RNA were indistinguishable from those of the non- or water-injected control cells. Voltage steps between -100 and $+100$ mV (in 10-mV increments) elicited identical currents in both oocyte populations, corresponding to the endogenous oocyte channel activity. [At $+50$ mV, 300 ms after the beginning of the voltage step, the current amplitudes were 0.28 ± 0.04 μA ($n = 8$) in the Kv8.2 RNA injected group and 0.27 ± 0.06 μA ($n = 7$) in the control group.] Because the amino acid sequence of Kv8.2 showed the characteristics of silent subunits, we examined the effects of Kv8.2 coexpression on Kv2.1 current. The expression of Kv2.1 alone induced high-amplitude voltage-dependent K^+ current (24.5 ± 6.4 μA, $n = 5$). When cRNAs encoding Kv8.2 and Kv2.1 were coinjected in a 1:1 ratio, Kv8.2 suppressed the Kv2.1 current (1.9 ± 0.4 μA, $n = 5$, $P < 0.01$).

To exclude the possibility that the expression of Kv8.2 saturated the expressing capacity of the oocyte, the inhibitory effect was also tested in oocytes coexpressing both Kv2.1 and a distantly related inward rectifier K^+ channel subunit, GIRK4m [a mutant GIRK4 (Kir3.4, KCNJ5) subunit; see METHODS for details]. Kv and GIRK currents were measured with different experimental protocols in the same oocyte. The oocytes coinjected with Kv2.1 and GIRK4m cRNAs coexpressed both currents (Fig. 3, *A* and *B*). Additional coexpression of Kv8.2 (triple coexpression) abolished the Kv2.1 current, but did not influence the GIRK4m current (Fig. 3, *C* and *D*). Thus Kv8.2 interacts with Kv2.1 specifically and does not block the expression of potassium channel subunits in general.

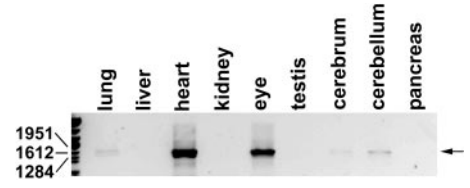

FIG. 1. Expression of Kv8.2 in different mouse tissues. Reverse transcriptase polymerase chain reaction (RT-PCR) was performed on total RNA purified from the indicated tissues. Specific 1,662-base pair (bp) PCR products are marked by an arrow.

Coexpression of Kv8.2 with Kv2.1 in an appropriate ratio results in a current with novel characteristics

To reveal functional heteromers, the expression and characteristics of voltage-dependent K^+ currents were examined in oocytes coinjected with Kv2.1 and Kv8.2 cRNAs in different ratios. If the ratio of Kv8.2 was decreased gradually, the degree of inhibition of the voltage-dependent current faded, but the emerging current showed characteristics different from those of Kv2.1 (see following text). However, when the ratio of Kv8.2 to Kv2.1 fell below 1:4, characteristic Kv2.1 current began to dominate, suggesting that the small percentage of Kv8.2 could not prevent the formation of functionally intact Kv2.1 homotetramers. In oocytes coinjected with Kv8.2 and Kv2.1 cRNAs in a ratio of 1:4, the steady-state activation curve was shifted to more negative potentials than in cells expressing Kv2.1 (for Kv2.1, $V_{1/2} = 7.8$ mV; for Kv2.1/Kv8.2, $V_{1/2} = -2.8$ mV, $P < 10^{-5}$; Fig. 4*A*). The activation threshold of the K^+ current was more negative (≈ -40 mV) than that in oocytes expressing only Kv2.1 (≈ -20 mV).

The voltage dependences of steady-state inactivation of Kv2.1 and Kv2.1/Kv8.2 were not significantly different ($V_{1/2} = -28.3$ and -30.6 mV, respectively; Fig. 4*A*). Negative shift of the steady-state activation with unaltered voltage-dependent inactivation resulted in a window current in oocytes coexpressing Kv2.1 and Kv8.2. Accordingly, the resting membrane potential of oocytes coexpressing both Kv subunits was more negative (-40.6 ± 0.9 mV, $n = 19$) than that of the cells expressing Kv2.1 alone (-31.5 ± 1.1 mV, $n = 23$, $P < 10^{-6}$). (The membrane potential of noninjected oocytes equaled that of the Kv2.1 group, -29.0 ± 0.6 mV, $n = 3$.)

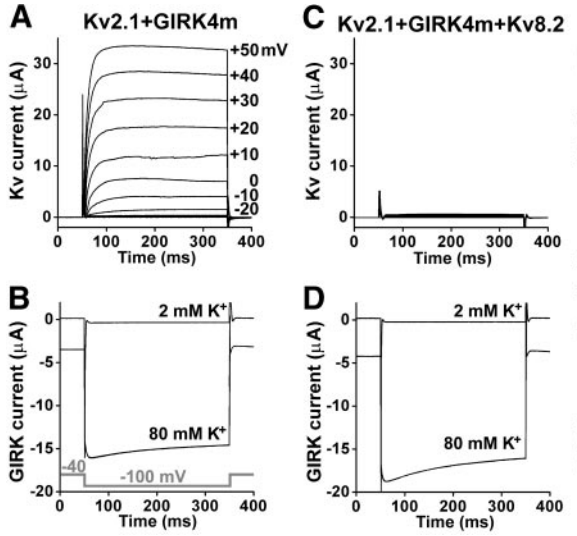

FIG. 3. In *Xenopus* oocytes coexpressing both Kv2.1 and GIRK4m, the Kv2.1 current is reduced selectively by the additional coexpression of Kv8.2. *A*: voltage-dependent K^+ currents of a representative *Xenopus* oocyte coexpressing Kv2.1 and GIRK4m (GIRK4 S143T mutant). Voltage steps of 300-ms duration were applied from −80 to +50 mV in 10-mV increments from a holding potential of −80 mV in 2 mM extracellular [K^+]. *B*: G-protein–coupled inwardly rectifying K^+ (GIRK) current of the same oocyte as on *A*. GIRK current was estimated as the difference of the inward currents in 80 and 2 mM extracellular [K^+]. Currents were measured at the end of 300-ms voltage steps to −100 mV from a holding potential of −40 mV. *C*: voltage-dependent K^+ currents of a representative *Xenopus* oocyte coexpressing Kv2.1, GIRK4m, and Kv8.2 (triple coexpression). (Methods of measurement and representation are identical to those in *A*.) *D*: GIRK currents of the same oocyte as on *C*. (Methods of measurement and representation are identical to those in *B*.) *E*: statistical evaluation of the voltage-dependent (Kv, dark bars) and GIRK (light bars) currents of the oocytes coexpressing Kv2.1 and GIRK4m or coexpressing Kv2.1, GIRK4m, and Kv8.2.

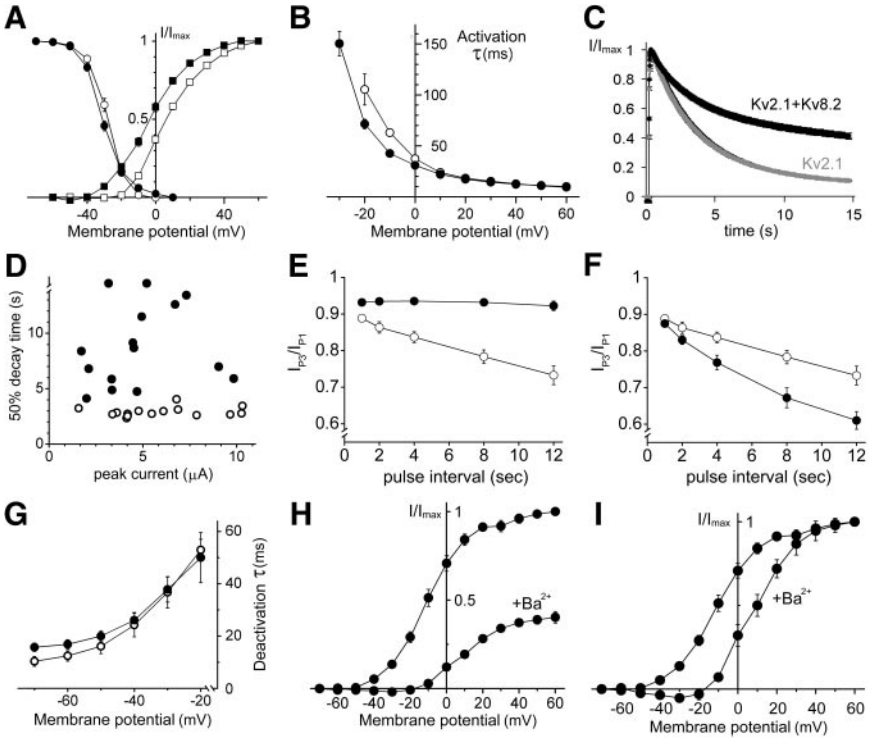

FIG. 4. Voltage- or time dependence of the activation, deactivation, inactivation, and barium sensitivity of Kv2.1/Kv8.2 heteromeric channels. *A*: voltage dependence of the steady-state activation (□, ■) and inactivation (○, ●) of the K^+ currents measured in oocytes expressing Kv2.1 [□ ($n = 19$), ○ ($n = 8$)] or coexpressing Kv2.1 and Kv8.2 [■ ($n = 11$), ● ($n = 5$)]. *B*: voltage dependence of the time constants of activation in oocytes expressing Kv2.1 (○, $n = 19$) or coexpressing Kv2.1 and Kv8.2 (●, $n = 16$). *C*: time course of inactivation during a voltage step to +40 mV from a holding potential of −80 mV in oocytes expressing Kv2.1 (gray symbols, $n = 17$) or coexpressing Kv2.1 and Kv8.2 (black symbols, $n = 15$). Recordings were normalized to their peak amplitudes, and the plotted curves correspond to mean ± SE. *D*: time required for the K^+ current to decay to 50% of the peak amplitude (during inactivation at +40 mV as in *C*) was plotted as the function of the peak current amplitude in oocytes expressing Kv2.1 (○) or coexpressing Kv2.1 and Kv8.2 (●). (In 2 cells inactivation did not reach 50% in 14.5 s.) *E*: closed-state inactivation was estimated by a protocol consisting of 3 successive voltage steps (P1, P2, and P3). Amount of channels available for activation was measured by 2 short identical depolarizations before (P1) and after (P3) the inactivating period (P2) of varying duration (see METHODS for details). Potential of the inactivating period was chosen to be 10 mV more negative than the threshold of activation of the K^+ current; −30 mV in oocytes expressing Kv2.1 and −50 mV in oocytes coexpressing Kv2.1 and Kv8.2. Current evoked by P3 was normalized to the value obtained from P1 and plotted as the function of duration of P2 in the case of Kv2.1 homomers (○, $n = 5$) and Kv2.1/Kv8.2 heteromers (●, $n = 5$). *F*: a similar experiment as in *E*, but both the Kv2.1 homomeric (○, $n = 5$) and Kv2.1/Kv8.2 heteromeric (●, $n = 5$) channels were inactivated at −30 mV (during P2). (Kv2.1 data points of *E* were repeated.) *G*: voltage dependence of the time constants of deactivation in oocytes expressing Kv2.1 (○, $n = 9$) or coexpressing Kv2.1 and Kv8.2 (●, $n = 8$). *H*: voltage dependence of the steady-state activation of the K^+ current in the absence or presence of 5 mM Ba^{2+} in oocytes coexpressing high amounts of Kv2.1 and Kv8.2 ($n = 6$). Channels were activated at different potentials by a prepulse of 200-ms duration, and the amplitudes of the subsequent tail currents (at −40 mV) were normalized to the maximum value measured after the +60-mV prepulse in the absence of Ba^{2+}. *I*: another representation of the experiment described in *H*. Tail currents were normalized to the respective maximum value measured in the absence or presence of Ba^{2+} after the +60-mV prepulse.

Currents of oocytes coexpressing Kv2.1 and Kv8.2 activated more quickly (especially at negative potentials) than those expressing Kv2.1 alone ($P < 0.005$ at -10 and -20 mV; Fig. 4*B*). There was also a significant difference between the kinetics of inactivation in the two groups; the current of the oocytes expressing Kv2.1/Kv8.2 inactivated more slowly ($P < 10^{-6}$; Fig. 4*C*). In this experiment (as in all the preceding cases of comparing Kv2.1 and Kv2.1/Kv8.2 groups) special care was taken to use oocytes expressing similar peak K^+ current amplitudes. Thus the slower inactivation in the Kv2.1/Kv8.2 group was independent from the peak current amplitude (Fig. 4*D*). Members of the Kv2 family were shown to inactivate from intermediate closed states, and the modulatory subunit Kv9.3 was demonstrated to substantially accelerate this inactivation. Therefore we examined how the coexpression of Kv8.2 influenced the closed-state inactivation of Kv2.1. The oocytes were depolarized to a value 10 mV more negative than the activation threshold of their expressed current. Kv2.1 exhibited a slight time-dependent inactivation in response to a prolonged depolarization to -30 mV. On the contrary, Kv2.1/Kv8.2 failed to inactivate at -50 mV (Fig. 4*E*). Therefore in contrast to Kv9.3, the coexpression of Kv8.2 does not accelerate the closed-state inactivation of Kv2.1. [Even if both currents were tested at -30 mV (above the activation threshold of Kv2.1/Kv8.2 but below that of Kv2.1), the inactivation of Kv2.1/Kv8.2 was only slightly quicker than that of Kv2.1 (Fig. 4*F*). This kinetics was in good agreement with the minor difference of the final (steady-state) inactivation at -30 mV after 1 min (Fig. 4*A*).]

Deactivation of Kv2.1/Kv8.2 was measured as the amplitude of the tail current at different potentials, after a 300-ms prepulse to $+60$ mV in 80 mM EC [K^+]. The rate of deactivation was similar to that of Kv2.1, when it was measured at depolarized potentials (-20 and -40 mV), and it became slightly (but significantly, $P < 0.03$) slower (compared with Kv2.1) at more negative (-70 to -50 mV) potentials (Fig. 4*G*). Considering that Kv2.1/Kv8.2 channels are never exposed to $+60$ mV under physiological circumstances, we also examined a more relevant parameter: their current relaxations during a voltage step from -30 to -40 mV in 2 mM extracellular [K^+] (recordings not shown). At these membrane potentials Kv2.1 homotetramer channels are not activated at all and only a small fraction of Kv2.1/Kv8.2 channels is in the open state. Activation and deactivation of Kv2.1/Kv8.2 can proceed with comparable time constants at both of these potentials (Fig. 4, *B* and *G*). The current relaxations during steps from -30 to -40 mV were well fitted with monoexponetials having very high time constants ($\tau = 237 \pm 11$ ms, $n = 5$).

Kv2.1/Kv8.2 current has pharmacological characteristics similar to those of I_{Kx}

It has been reported that the unique potassium current of amphibian rods (I_{Kx}) can be distinguished from other currents by taking advantage of its insensitivity to Cs^+ and Cd^{2+} (Beech and Barnes 1989). In the present experiments, combined application of 5 mM Cs^+ and 100 μM Cd^{2+} also failed to influence the Kv2.1/Kv8.2 current (at $+60$ mV the peak current amplitudes were reduced by $2.2 \pm 0.8\%$, $n = 4$). Ba^{2+} was found to inhibit I_{Kx} in tiger salamander rods in an unusual and unique manner; in addition to the reduction of the current amplitudes, the steady-state voltage-dependent activation was shifted to more positive potentials (Beech and Barnes 1989; Wollmuth 1994). Kv2.1/Kv8.2 was blocked in the same way; 5 mM Ba^{2+} reduced the tail current by 60% (at $+60$-mV activating prepulse; Fig. 4*H*) and $V_{1/2}$ of the steady-state voltage-dependent activation was shifted from -9.7 to 10.5 mV (Fig. 4*I*). Similarly to the previous observations on I_{Kx} (Wollmuth 1994), this Ba^{2+}-induced shift of the activation curve was measured in the presence of 3 mM EC [Ca^{2+}], and the effect of Ba^{2+} could not be mimicked by further elevating EC [Ca^{2+}] to 8 mM (data not shown).

Kv2.1/Kv8.2 induces amplified hyperpolarization in response to quick reduction of inward current

It has been suggested that the voltage-dependent K^+ current of amphibian rods (I_{Kx}) generates a hyperpolarizing overshoot of the membrane potential at the onset of light, which exceeds the level of hyperpolarization evoked by persistent illumination. We questioned whether the properties of Kv2.1/Kv8.2 enable the heteromer to contribute to this mechanism. Therefore under current-clamp conditions, we injected a constant inward current of 200 nA into oocytes coexpressing Kv2.1 and Kv8.2 (as an equivalent of the dark current of rods through the open CNG channels). After the stabilization of the membrane potential (near -30 mV), the current was abruptly switched off (Fig. 5*A*). The membrane potential transiently hyperpolarized far below the resting value (approximating -60 mV in the

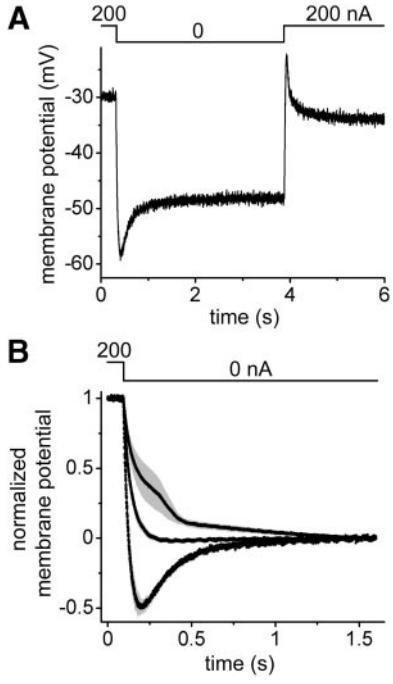

FIG. 5. Quick reduction of inward current evokes hyperpolarizing overshoot of the membrane potential in oocytes coexpressing Kv2.1 and Kv8.2. *A*: membrane potential alterations during successive current steps from 200 to 0 nA and back in an oocyte coexpressing Kv2.1 and Kv8.2 (representative 2-electrode current-clamp experiment). *B*: normalized membrane potential responses to a current step from 200 to 0 nA in oocytes expressing Kv2.1 (*top curve*, $n = 6$), TASK-1 (*middle curve*, $n = 6$), or coexpressing Kv2.1 and Kv8.2 (*bottom curve*, $n = 5$). Light gray areas around the curves represent SE. Steady-state membrane potential during the inward injection of 200 nA was normalized to 1. Membrane potential measured 1.5 s after the termination of the current injection was normalized to 0.

representative experiment) and reached the resting level (i.e., the steady-state membrane potential in the absence of injected inward current, around −50 mV) only after the cessation of this overhyperpolarization. When the 200-nA inward current was switched on again, a similar overshoot of the membrane potential occurred, but now in the depolarizing direction (Fig. 5*A*).

The hyperpolarizing overshoot of the membrane potential was not detected in oocytes expressing only Kv2.1 or the background (leak) K^+ channel, TASK-1 (Fig. 5*B*). In the cells expressing only Kv2.1, the membrane potential stabilized at highly positive values (near +30 mV) during the injection of 200-nA inward current because Kv2.1 inactivated entirely after a while and thus could not produce an opposing sustained outward current. After turning off the 200-nA inward current, the membrane potential slowly returned to the resting level, presumably depending on the endogenous oocyte currents. In the other control group, the sustained outward current of TASK-1 permanently prevented extreme depolarization. However, TASK-1 is a leak channel, which does not activate and deactivate voltage dependently (Duprat et al. 1997). Accordingly, its current instantaneously followed the changes of the membrane potential and this excluded the overshoot phenomenon.

Kv8.2 G476D mutant has dominant negative effect on Kv2.1

In humans different Kv8.2 mutants were found to be associated with "cone dystrophy with supernormal rod electroretinogram." The mouse equivalent of a pore domain mutant, G476D was constructed and its effect on Kv2.1 was tested. Coexpression of equal amounts of Kv8.2 G476D with Kv2.1 abolished the current of the latter (Fig. 6*A*). When the ratio of the mutant channel was lower (the same as the ratio giving rise to the modified currents in the case of the wild-type subunits), a current appeared. However, the characteristics of this current could not be distinguished from those of Kv2.1 homotetramers (Fig. 6, *B* and *C*). The negative shift of the resting membrane potential of the oocytes expressing the mutant was missing [−31.8 ± 1.4 and −29.8 ± 1.9 mV in oocytes expressing Kv2.1 and Kv2.1/Kv8.2 G476D, respectively (both $n = 5$)].

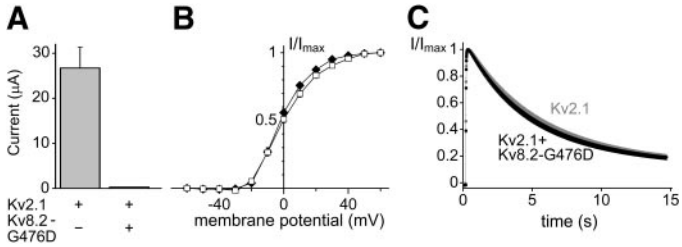

FIG. 6. Coexpression of the pore domain mutant Kv8.2 G476D with Kv2.1 can diminish the K^+ current but does not affect the voltage dependence of activation and the time-dependent inactivation. *A*: voltage-dependent K^+ current was induced by a 300-ms depolarizing step to +50 mV in oocytes injected with Kv2.1 cRNA ($n = 5$, *left column*) or coinjected with the same amount of Kv2.1 and Kv8.2 G476D cRNAs ($n = 5$, *right column*). (*Right column* is barely visible because of the almost complete elimination of the K^+ current.) *B*: voltage dependence of the steady-state activation of the K^+ current in oocytes expressing Kv2.1 (□, $n = 5$) or coexpressing Kv2.1 with a reduced amount of Kv8.2 G476D (◆, $n = 5$). *C*: time course of inactivation in oocytes expressing Kv2.1 (gray symbols, $n = 5$) or coexpressing Kv2.1 and Kv8.2 G476D (black symbols, $n = 5$). (Methods of measurement and representation are identical to those in Fig. 4*C*.)

The steady-state activation curve and the time-dependent inactivation were indistinguishable in the presence or absence of Kv8.2 G476D. These observations indicate that Kv8.2 G476D does not form functional heteromers with Kv2.1, although this mutant eliminates Kv2.1 current in a dominant negative manner.

DISCUSSION

In the present study we report the cloning of Kv8.2 voltage-dependent potassium channel subunit from mouse eye. It is supported by several lines of evidence that Kv8.2 is expressed abundantly in the retina. Most expressed sequence tag (EST) data corresponding to Kv8.2 originate from mouse or human eye (in most cases retina) cDNA libraries. By RT-PCR, the highest amount of Kv8.2 PCR product was amplified from mouse eye and heart. The radioactive Kv8.2-specific antisense RNA probe highlighted the circumference of the eye in a whole perinatal rat section. This massive signal was localized to the outer nuclear layer (ONL) consisting of nuclei and cell bodies of photoreceptor cells. Because the cones are sparse in the retina of rodents pursuing nightlife, and they are located mainly at the outer edge of the ONL (Blanks and Johnson 1983; Rich et al. 1997), the intense, homogeneous labeling of the ONL indicated that, in the mouse, Kv8.2 was expressed in rods.

The primary structure of Kv8.2 suggests that it is a silent Kv subunit. Accordingly, it does not induce K^+ current on its own, but interacts specifically with Kv2.1 in *Xenopus* oocytes. The coexpression of high amounts of Kv8.2 specifically eliminated the Kv2.1 current in our experiments, whereas the same Kv8.2 coexpression did not affect the current of GIRK4m, a structurally unrelated inwardly rectifying K^+ channel. If a lower amount of Kv8.2 was coexpressed with Kv2.1, a voltage-dependent current with novel properties emerged. With respect to the formation of heteromeric channels from Kv2.1 and Kv8.2 subunits, our functional data are in good agreement with the coimmunoprecipitation results obtained in the case of human Kv8.2 and Kv2.1 (Ottschytsch et al. 2002). However, in the human Kv8.2 study, in mouse L cells lacking thymidine kinase (Ltk−cells), the suppressing effect of Kv8.2 coexpression on the Kv2.1 current has not been reported. The lack of such a suppressing effect would be unusual because the diminished current amplitudes were consistently observed both in mammalian cell lines and in *Xenopus* oocytes, when Kv2.1 and different modulatory subunits were coexpressed in equal amounts (Castellano et al. 1997; Hugnot et al. 1996; Salinas et al. 1997b; Stocker et al. 1999). Furthermore, it was clearly demonstrated by combined electrophysiological and FRET (fluorescence resonance energy transfer) measurements that a stochiometry of 3:1 was necessary to obtain functional heteromers of Kv2.1 and Kv9.3, and a higher proportion of Kv9.3 resulted in the accumulation of nonfunctional Kv2.1/Kv9.3 heterodimers (Kerschensteiner et al. 2005).

There is an even more important discrepancy between the reported electrophysiological properties of human Kv8.2 and our data, substantially affecting the appreciation of the function of Kv2.1/Kv8.2 heteromer. In the previous report about the human channel, Kv8.2 was found to shift both the steady-state voltage-dependent activation and inactivation curves of Kv2.1 by −5 mV (Ottschytsch et al. 2002). These parallel changes

would merely affect the voltage dependence of repolarization. In contrast to this earlier report, our results indicate that Kv8.2 shifts the steady-state activation of Kv2.1 to more negative potentials, but leaves the voltage dependence of steady-state inactivation unaltered. This apparently minor discrepancy results in fundamentally different properties and provides potential function for Kv2.1/Kv8.2. Activation, inactivation, and recovery from inactivation of Kv2.1/Kv8.2 may occur in a membrane potential range (window) delimited by the steady-state activation and inactivation curves, and a persistent fraction of the channels may be in the open state at a given potential in this range (about −40 to −10 mV). In addition, the Kv2.1/Kv8.2 heteromer channel does not show accelerated closed-state inactivation, which is a characteristic for the heteromer of Kv2.1 and another modulatory subunit, Kv9.3 (Kerschensteiner and Stocker 1999). Therefore Kv2.1/Kv8.2 cannot circumvent the open state; the channel has to open before it can inactivate. As a consequence of these fine-tuned electrophysiological properties, Kv2.1/Kv8.2, in contrast to Kv2.1 homomeric channels, produces a permanent outward K^+ current within the membrane potential range characteristic for the photoreceptor cells.

We also found that Kv2.1/Kv8.2 heteromer activated faster at physiologically relevant membrane potentials and inactivated more slowly than Kv2.1 homomer. The deactivation time constants of Kv2.1/Kv8.2 are high, similarly to Kv2.1 homomeric channels (they are in the range of 10–60 ms, depending on the membrane potential); i.e., both of them deactivate slowly. Moreover, the current relaxation of Kv2.1/Kv8.2 during hyperpolarizing membrane potential changes within the window current range is even slower than would be expected on the basis of the deactivation time constants because the continuous activation of Kv2.1/Kv8.2 can counteract the deactivation process. The very slow current decay during a voltage step from −30 to −40 mV ($\tau = 237 \pm 11$ ms, $n = 5$) corresponds well to the current relaxation of I_{Kx} ($\tau = 250$ ms) measured by an identical protocol in the rods of aquatic tiger salamanders (Beech and Barnes 1989). The functional importance of this slow relaxation of the K^+ current in photoreceptor cells was emphasized by several studies.

In response to illumination of rapid onset, the intracellular cGMP concentration drops, the inward current of the cyclic-nucleotide-gated (CNG) channels quickly decreases, and the photoreceptor cell hyperpolarizes. Because of their slow deactivation, the K^+ channels of the photoreceptor cell close after a relatively long delay. Therefore the outward K^+ current remains larger than the inward current through the CNG channels for a period, the length of which is determined by the relaxation of the K^+ current. During this initial period, the K^+ conductance is higher than that after closure of the K^+ channels; thus the membrane is hyperpolarized transiently to a more negative potential than the value characteristic for steady illumination. This hyperpolarizing overshoot has an important role in increasing the sensitivity to rapid changes of illumination. If the illumination intensifies slowly (and thus the decrease of the inward current through the CNG channels is slow) compared with the deactivation of the K^+ current (representing a low-frequency change), then the K^+ channels have enough time to close and the hyperpolarizing overshoot of membrane potential does not occur. Therefore only the sufficiently quick reductions of inward current evoke high-amplitude transient hyperpolarizations; accordingly, the photoreceptor cell functions like a high-pass amplifier (Baylor et al. 1984; Demontis et al. 1999; Detwiler et al. 1978; Owen and Torre 1983; Torre and Owen 1983). [This mechanism is complemented by the hyperpolarization-activated nonspecific cation current I_h, which sharpens the hyperpolarizing peak by its delayed activation (Beech and Barnes 1989; Demontis et al. 1999).]

Three electrophysiological characteristics of a K^+ channel are required for the high-pass amplifier effect. The channel has to be voltage dependent, it has to produce permanent K^+ current at depolarized potentials, and it has to deactivate slowly. Because Kv2.1/Kv8.2 fulfilled these criteria, we examined whether the high-pass amplifier mechanism was reproduced in *Xenopus* oocytes expressing the heterodimer. Kv2.1 homomeric channels and a leak K^+ channel, TASK-1, were used as controls. In these experiments, the dark current of CNG channels was "substituted" with the experimentally controlled inward current of two-electrode current clamp. Despite the substantial capacitance of the oocyte, Kv2.1/Kv8.2 could produce a nearly 50% hyperpolarizing overshoot exceeding the (zero-current steady-state) resting membrane potential, after the sudden cessation of an inward current of 200 nA. No hyperpolarizing overshoot developed in our control oocytes expressing Kv2.1 homomers or TASK-1. Although Kv2.1 homomers are voltage dependent and deactivate slowly, they cannot produce permanent current at depolarized membrane potentials. The injection of the inward current of 200 nA induced depolarization, taking all the Kv2.1 channels to the inactivated state in the end. These inactivated channels did not influence the membrane potential, when the injection of inward current ceased. In turn, TASK-1 channels produced permanent current at depolarized membrane potential, but their current instantaneously followed the changes of membrane potential (Millar et al. 2000) because the membrane potential determined only the driving force for K^+, but not the TASK-1 activity. Therefore after the cessation of the depolarizing inward current, when the membrane potential approached the value characteristic for the steady state, TASK-1 channels did not further conduct excess transient current. Only Kv2.1/Kv8.2 had the essential characteristics required for the high-pass amplifier effect: the sustained outward current and slow deactivation. These characteristics and our results obtained in the *Xenopus* system indicate that Kv2.1/Kv8.2 can efficiently induce the high-pass amplifier effect in the cells in which it is expressed.

The high-level expression of Kv8.2 (together with Kv2.1) in the retina and its electrophysiological properties suggest that Kv2.1/Kv8.2 may contribute to the generation of the K^+ current responsible for the dynamic signal amplification of photoreceptor cells. Previous works already attempted to identify the channels inducing this unique potassium current, but they failed to provide consistent results. The first candidate, the M current, resembled the K^+ current of amphibian rods (I_{Kx}) with respect to the similar voltage dependence of activation (Wollmuth 1994). However, it did not display the special sensitivity of I_{Kx} to Ba^{2+}, which includes not only the suppression of tail-current amplitudes, but also the unique shift of voltage-dependent steady-state activation to more positive potentials (an effect that cannot be reproduced by elevating EC $[Ca^{2+}]$; Wollmuth 1994). Later, the mammalian equivalent of *Drosophila ether-à-go-go* channel (*eag*) was suggested as a

possible candidate (Frings et al. 1998). Although *eag* shares some characteristics of I_{Kx} (it activates at negative membrane potentials, from −50 mV, and does not inactivate), it strikingly differs in other, functionally important respects. Slow deactivation of I_{Kx} is one of the most characteristic and functionally important features of the current. As opposed to I_{Kx}, *eag* deactivates completely in a few milliseconds and Ba^{2+} does not shift its voltage-dependent activation curve (Frings et al. 1998). Thus it is unlikely that *eag* is a major component of the rod K^+ current (at any rate in the amphibian retina), and the role of *eag* in the dynamic signal amplification is theoretically rather ambiguous.

Examination of Kv channel expression in the retina by in situ hybridization showed a high abundance of Kv2.1 (drk1; Frech et al. 1989) mRNA in rods, and the channel protein was localized to the inner segment by immunohistochemistry (Klumpp et al. 1995). Despite these data, the functional relation between Kv2.1 and the characteristic K^+ current of photoreceptor cells has never been anticipated because of the apparent inconsistency of the electrophysiological properties of the two currents. Kv2.1 opens only above −20 mV (Frech et al. 1989), which is outside the normal membrane potential range (−30 to −70 mV) of photoreceptor cells (Werblin 1975). In addition, Kv2.1 inactivates. Apparently, this was another argument against the role of Kv2.1 in the generation of a sustained outward current. The heteromerization with Kv8.2 clarifies the reason that Kv2.1 is expressed in the photoreceptor cells.

Despite the large filogenetic distance between rodents and amphibians, the pharmacological profile of Kv2.1/Kv8.2 corresponds surprisingly well to that of I_{Kx}, the most extensively studied photoreceptor K^+ current. Both currents are insensitive to Cs^+ and Cd^{2+}, which ions were extensively used in salamander rods to discriminate I_{Kx} from the other currents. However, the most impressive is the inhibition of Kv2.1/Kv8.2 current by Ba^{2+}. Ba^{2+} not only is inhibitory in the same concentration range, but also induces the shift of the voltage-dependent steady-state activation curve to more positive potentials. None of the previous candidates for I_{Kx} exhibited this property to our knowledge. Kv2.1/Kv8.2 also possesses similar kinetics of activation, inactivation, and current relaxation as I_{Kx}. There is only one apparent difference between the two currents. I_{Kx} in amphibian photoreceptor cells has an activation threshold of −60 mV, whereas this value for Kv2.1/Kv8.2 expressed in *Xenopus* oocytes is about −40 mV. At present, the cause of this difference is unknown, but in addition to the species difference, another plausible explanation may be that Kv2.1/Kv8.2 is not the only constituent of the photoreceptor K^+ current, but it is coexpressed with other voltage-gated K^+ channels (e.g., *eag* or M current), and thus the activation threshold of the ensemble current is shifted to more negative values.

In a recent report (Wu et al. 2006) different mutations of the KCNV2 (Kv8.2) gene were linked to "cone dystrophy with supernormal rod electroretinogram" (with autosomal recessive inheritance). Some of these mutations resulted in the early termination of the coded protein (e.g., the nonsense mutation at the third lysine). These mutations most probably eliminated the expression of Kv8.2 and, consequently, all of its functions too. In other cases, the position of the point mutation suggested that the resulting mutant subunits were not functional as a K^+ channel. One of these human mutations (G459D) was localized to the K^+ channel signature sequence. To examine the effects of this mutant subunit, we constructed the mouse version of the same mutation, G476D. Kv8.2 G476D eliminated the Kv2.1 current, if the subunits were coexpressed in equal amounts. If the proportion of the coexpressed Kv8.2 G476D was reduced sufficiently then the emerging small current was indistinguishable from that of Kv2.1 homotetramers, indicating that Kv8.2 G476D did not participate in the formation of functional channels with its crippled pore domain. The clinical data indicated that both the complete absence of Kv8.2 (in which case the function of Kv2.1 channels is unaffected) and its mutation to a dominant negative form (which interferes with Kv2.1 activity similarly to the wild-type, but which does not form functional channels) result in the same degenerative visual defect (Wu et al. 2006). This suggests that it is the special current of Kv2.1/Kv8.2 heteromeric channels—and not only the reduction of Kv2.1 function—that is required for the functional integrity in the photoreceptor cells.

ACKNOWLEDGMENTS

We thank Professor M. Lazdunski, Dr. F. Lesage, and Dr. C. Girard for the pEXO, pEXO-TASK-1, and pCIrKv2.1 plasmids; and Dr. T. Rohács and Professor D. Logothetis for pGEMHE-GIRK4-S143T. The skillful technical assistance of I. Veres and B. Busi is highly appreciated.

GRANTS

This work was supported by Hungarian National Research Fund Grants OTKA T-046954, T-043169, and F-67743, Hungarian Medical Research Council Grant ETT-417/206, and a Semmelweis University Research Grant. G. Czirják was supported by a János Bolyai fellowship of the Hungarian Academy of Sciences.

REFERENCES

Baylor DA, Matthews G, Nunn BJ. Location and function of voltage-sensitive conductances in retinal rods of the salamander, *Ambystoma tigrinum*. *J Physiol* 354: 203–223, 1984.

Beech DJ, Barnes S. Characterization of a voltage-gated K^+ channel that accelerates the rod response to dim light. *Neuron* 3: 573–581, 1989.

Blanks JC, Johnson LV. Selective lectin binding of the developing mouse retina. *J Comp Neurol* 221: 31–41, 1983.

Bradley DJ, Towle HC, Young WS. Spatial and temporal expression of alpha- and beta-thyroid hormone receptor mRNAs, including the beta 2-subtype, in the developing mammalian nervous system. *J Neurosci* 12: 2288–2302, 1992.

Castellano A, Chiara MD, Mellstrom B, Molina A, Monje F, Naranjo JR, Lopez-Barneo J. Identification and functional characterization of a K^+ channel alpha-subunit with regulatory properties specific to brain. *J Neurosci* 17: 4652–4661, 1997.

Coetzee WA, Amarillo Y, Chiu J, Chow A, Lau D, McCormack T, Morena H, Nadal MS, Ozaita A, Pountney D, Saganich M, Vega-Saenz de Miera E, Rudy B. Molecular diversity of K^+ channels. *Ann NY Acad Sci* 868: 233–255, 1999.

Czirják G, Enyedi P. Formation of functional heterodimers between the TASK-1 and TASK-3 two-pore domain potassium channel subunits. *J Biol Chem* 277: 5426–5432, 2002.

Demontis GC, Longoni B, Barcaro U, Cervetto L. Properties and functional roles of hyperpolarization-gated currents in guinea-pig retinal rods. *J Physiol* 515: 813–828, 1999.

Detwiler PB, Hodgkin AL, McNaughton PA. A surprising property of electrical spread in the network of rods in the turtle's retina. *Nature* 274: 562–565, 1978.

Duprat F, Lesage F, Fink M, Reyes R, Heurteaux C, Lazdunski M. TASK, a human background K^+ channel to sense external pH variations near physiological pH. *EMBO J* 16: 5464–5471, 1997.

Fantozzi I, Platoshyn O, Wong AH, Zhang S, Remillard CV, Furtado MR, Petrauskene OV, Yuan JXJ. Bone morphogenetic protein-2 upregulates expression and function of voltage gated K^+ channels in human pulmonary

artery smooth muscle cells. *Am J Physiol Lung Cell Mol Physiol* 291: L993–L1004, 2006.

Frech GC, VanDongen AM, Schuster G, Brown AM, Joho RH. A novel potassium channel with delayed rectifier properties isolated from rat brain by expression cloning. *Nature* 340: 642–645, 1989.

Frings S, Brull N, Dzeja C, Angele A, Hagen V, Kaupp UB, Baumann A. Characterization of ether-a-go-go channels present in photoreceptors reveals similarity to I_{Kx}, a K^+ current in rod inner segments. *J Gen Physiol* 111: 583–599, 1998.

Horváth A, Szabadkai G, Várnai P, Arányi T, Wollheim CB, Spät A, Enyedi P. Voltage-dependent calcium channels in adrenal glomerulosa cells and in insulin producing cells. *Cell Calcium* 23: 33–42, 1998.

Hugnot JP, Salinas M, Lesage F, Guillemare E, de Weille J, Heurteaux C, Mattei MG, Lazdunski M. Kv8.1, a new neuronal potassium channel subunit with specific inhibitory properties towards Shab and Shaw channels. *EMBO J* 15: 3322–3331, 1996.

Kerschensteiner D, Soto F, Stocker M. Fluorescence measurements reveal stoichiometry of K^+ channels formed by modulatory and delayed rectifier alpha-subunits. *Proc Natl Acad Sci USA* 102: 6160–6165, 2005.

Kerschensteiner D, Stocker M. Heteromeric assembly of Kv2.1 with Kv9.3: effect on the state dependence of inactivation. *Biophys J* 77: 248–257, 1999.

Klumpp DJ, Song EJ, Pinto LH. Identification and localization of K^+ channels in the mouse retina. *Vis Neurosci* 12: 1177–1190, 1995.

Kramer JW, Post MA, Brown AM, Kirsch GE. Modulation of potassium channel gating by coexpression of Kv2.1 with regulatory Kv5.1 or Kv6.1 alpha-subunits. *Am J Physiol Cell Physiol* 274: C1501–C1510, 1998.

Li M, Jan YN, Jan LY. Specification of subunit assembly by the hydrophilic amino-terminal domain of the Shaker potassium channel. *Science* 257: 1225–1230, 1992.

Millar JA, Barratt L, Southan AP, Page KM, Fyffe RE, Robertson B, Mathie A. A functional role for the two-pore domain potassium channel TASK-1 in cerebellar granule neurons. *Proc Natl Acad Sci USA* 97: 3614–3618, 2000.

Ottschytsch N, Raes A, Van Hoorick D, Snyders DJ. Obligatory heterotetramerization of three previously uncharacterized Kv channel alpha-subunits identified in the human genome. *Proc Natl Acad Sci USA* 99: 7986–7991, 2002.

Owen WG, Torre V. High-pass filtering of small signals by retinal rods. Ionic studies. *Biophys J* 41: 325–339, 1983.

Patel AJ, Lazdunski M, Honore E. Kv2.1/Kv9.3, a novel ATP-dependent delayed-rectifier K^+ channel in oxygen-sensitive pulmonary artery myocytes. *EMBO J* 16: 6615–6625, 1997.

Post MA, Kirsch GE, Brown AM. Kv2.1 and electrically silent Kv6.1 potassium channel subunits combine and express a novel current. *FEBS Lett* 399: 177–182, 1996.

Rich KA, Zhan Y, Blanks JC. Migration and synaptogenesis of cone photoreceptors in the developing mouse retina. *J Comp Neurol* 388: 47–63, 1997.

Salinas M, de Weille J, Guillemare E, Lazdunski M, Hugnot JP. Modes of regulation of *Shab* K^+ channel activity by the Kv8.1 subunit. *J Biol Chem* 272: 8774–8780, 1997a.

Salinas M, Duprat F, Heurteaux C, Hugnot JP, Lazdunski M. New modulatory alpha subunits for mammalian *Shab* K^+ channels. *J Biol Chem* 272: 24371–24379, 1997b.

Shen NV, Pfaffinger PJ. Molecular recognition and assembly sequences involved in the subfamily-specific assembly of voltage-gated K^+ channel subunit proteins. *Neuron* 14: 625–633, 1995.

Sheng M, Liao YJ, Jan YN, Jan LY. Presynaptic A-current based on heteromultimeric K^+ channels detected in vivo. *Nature* 365: 72–75, 1993.

Stocker M, Hellwig M, Kerschensteiner D. Subunit assembly and domain analysis of electrically silent K^+ channel alpha-subunits of the rat Kv9 subfamily. *J Neurochem* 72: 1725–1734, 1999.

Stocker M, Kerschensteiner D. Cloning and tissue distribution of two new potassium channel alpha-subunits from rat brain. *Biochem Biophys Res Commun* 248: 927–934, 1998.

Torre V, Owen WG. High-pass filtering of small signals by the rod network in the retina of the toad, *Bufo marinus*. *Biophys J* 41: 305–324, 1983.

Vivaudou M, Chan KW, Sui JL, Jan LY, Reuveny E, Logothetis DE. Probing the G-protein regulation of GIRK1 and GIRK4, the two subunits of the KACh channel, using functional homomeric mutants. *J Biol Chem* 272: 31553–31560, 1997.

Wang H, Kunkel DD, Martin TM, Schwartzkroin PA, Tempel BL. Heteromultimeric K^+ channels in terminal and juxtaparanodal regions of neurons. *Nature* 365: 75–79, 1993.

Werblin FS. Regenerative hyperpolarization in rods. *J Physiol* 244: 53–81, 1975.

Wollmuth LP. Mechanism of Ba^{2+} block of M-like K^+ channels of rod photoreceptors of tiger salamanders. *J Gen Physiol* 103: 45–66, 1994.

Wu HM, Cowing JA, Michaelides M, Wilkie SE, Jeffery G, Jenkins SA, Mester V, Bird AC, Robson AG, Holder GE, Moore AT, Hunt DM, Webster AR. Mutations in the gene KCNV2 encoding a voltage-gated potassium channel subunit cause "cone dystrophy with supernormal rod electroretinogram" in humans. *Am J Hum Genet* 79: 574–579, 2006.

Young WS 3rd. In situ hybridization histochemical detection of neuropeptide mRNA using DNA and RNA probes. *Methods Enzymol* 168: 702–710, 1989.